https://doi.org/10.5194/egusphere-2024-3477
Preprint. Discussion started: 25 November 2024

Technical note: Automatic retrieval of wind speed and direction from in situ wave observations of a small buoy

Jan-Victor Björkqvist[1] and Victor Alari[2]

[1]Norwegian Meteorological Institute, Allégaten 70, 5007 Bergen, Norway
[2]Department of Marine Systems, Tallinn University of Technology, Akadeemia tee 15, 12618 Tallinn, Estonia

Correspondence: Jan-Victor Björkqvist (janvb@met.no)

Abstract. This study presents an automatic algorithm for estimating the wind speed and direction from wave observations. The method rests upon the decades old field-validated theory that the energy of a certain part of the wave field is directly proportional to the wind speed. The wind properties were estimated using data from a small wave buoy moored in the sheltered Finnish archipelago and in the exposed Baltic Proper (the Baltic Sea). The estimated wind speed and directions were compared to a nearby weather station (archipelago) and a high-resolution numerical hindcast (Baltic Proper). The algorithm was able to accurately estimate the wind speed (biases 0.3–0.5 $\mathrm{m\ s^{-1}}$ and root-mean-square-errors 1.5–1.6 $\mathrm{m\ s^{-1}}$). The wind direction was estimated from the mean wave direction of the shortest waves (1.00–1.28 Hz) and was mostly within 20° of the observed wind direction, with some of the differences clearly explained by land and coastlines tainting the measurements. As an additional measure to previously implemented algorithms, the estimated wind direction was used when determining the wind speed, which is expected to add robustness if strong swell is present. The results of the different places were obtained using slightly different equilibrium level constants, α_u, but with otherwise identical algorithm settings, which suggests that the difference is caused by a more fundamental uncertainty of the value of the experimental constant, not the details of the algorithm itself.

1 Introduction

There is an obvious connection between surface waves and the wind blowing over the sea. The total wave height is not determined by only the wind, but evidence suggest that a certain part of the wave field reach an equilibrium with the wind speed (e.g. Kahma, 1981). More exactly, the energy of waves of a certain length seems to be directly proportional to the wind speed; this finding has dimensional and theoretical foundations, and has been confirmed by experimental studies (e.g. Kahma, 1981; Forristall, 1981; Kitaigorodskii, 1983; Phillips, 1985; Resio et al., 2004).

While the general idea of this equilibrium range is not in question, the details of its characteristics are still unclear. While the wind speed itself (at a certain height) have described field data well, there exist powerful arguments for that the equilibrium range should actually scale with the friction velocity (e.g. Toba, 1973; Voermans et al., 2020). This, however, means that

https://doi.org/10.5194/egusphere-2024-3477
Preprint. Discussion started: 25 November 2024

connecting waves to the wind speed falls behind an additional layer of uncertainty, since the relation between the friction velocity and the wind depends on the boundary layer properties, and thus also on the stress carried by the roughness of the waves (e.g. Janssen, 1989).

Although the exact scientific details are unclear, we do have enough knowledge to estimate the wind speed from the wave spectrum derived from observations. This is evident from the thorough study of Voermans et al. (2020), where the wind speed was estimated from in situ wave observation using a solid theoretical framework for the air–sea boundary. The authors found that smaller buoys provided more accurate results, showing that the type of the measurement device is also an uncertainty. Later, Jiang (2022) used deep learning without any explicit theoretical assumptions to determine the wind speed from wave spectra.

Directly measuring the wind at sea is difficult, and we often rely on remote sensing and numerical models. Estimates from wave spectra – although not as accurate as in situ measurement – provide a third independent quantification of the wind. Since wave measurements are often easier to make, they can complement satellite products and numerical models in locations where in situ measurements might otherwise not exist. For example, an automatic wind speed retrieval algorithm has been implemented in the Sofar Spotter buoy.

This study focuses on implementing an automatic wind speed retrieval algorithm for a small in situ wave buoy (Alari et al., 2022). The implementation will use the simplest theoretical model for the equilibrium range, which is supported by a lot of field observations. While this may not be as theoretically elaborate as the work of Voermans et al. (2020), its simplicity is a major upside because the method is meant to be implemented as a real-time algorithm that will be calculated on board the in situ instrument.

This manuscript is structured as follows: Section 2 describes the model for the equilibrium range and the automatic algorithm. Section 3 presents the validation of the algorithm against field data, while Section 4 summarises the technical note and concludes the findings.

2 Materials and methods

2.1 Theoretical framework

The omnidirectional wave spectrum, $S(\omega)$ ($\mathrm{m^2 s}$) can be determined from a vertical displacement time series. It gives the variance of the wave field as a function of the angular frequency ω ($\mathrm{rad\,s^{-1}}$). The so called equilibrium range of the wave spectrum follows an ω^{-4} power law, and the wind speed (U) dependent expression follows from dimensional arguments:

$$S(\omega) = \alpha_u U g \omega^{-4}, \tag{1}$$

where α_u is an experimental constant and g ($\mathrm{m\ s^{-2}}$) is the acceleration due to gravity. As a starting point we take values that have been derived from field measurements, namely $3.3 \cdot 10^{-3}$ and $4.5 \cdot 10^{-3}$ (Kahma, 1981, 1986). Given an α_u, the wind speed can be deduced from the wave spectrum.

https://doi.org/10.5194/egusphere-2024-3477
Preprint. Discussion started: 25 November 2024

An exact definition for the equilibrium range doesn't exist, but the lowest frequency is slightly above the peak frequency (ω_p) and the upper bound is the transition to an ω^{-5} power law, which should be independent of the wind based on dimensional arguments (Phillips, 1958). This transition point is not exactly known, but happens around $\omega/\omega_p \approx 3$ (e.g. Banner, 1990; Resio et al., 2004).

The waves in the equilibrium range can be long enough to be affected by slanting fetch effects (e.g. Holthuijsen, 1983). The wind direction was therefore estimated from the shortest waves, regardless of if they followed Eq. 1 or not.

2.2 Algorithm

The wind direction is estimated from the shortest measured waves as:

$$U_d \approx \operatorname{atan}\frac{\langle a_1(\omega)\rangle}{\langle b_1(\omega)\rangle} + 180^\circ, \tag{2}$$

where $\langle\rangle$ denotes an average over the frequency interval $2\pi \cdot 1.00 - 2\pi \cdot 1.28$ rad s^{-1}, and a_1 and b_1 are the first Fourier coefficients (see e.g. Kuik et al., 1988).

The algorithm to estimate the wind speed has four steps. We need to determine:

1. a lowest frequency to start the search (denoted ω_0).
2. all possible frequency ranges of a certain length above ω_0.
3. one range, $\Delta\omega$, using some measure for the goodness-of-fit to step 2.
4. the wind speed using spectral density levels of $\Delta\omega$.

Step 1: The peak frequency, ω_p seems to be an obvious candidate. In practice, however, the peak might not be well defined, or the spectrum might be double peaked. We therefore also calculated the mean frequency (ω_m), and the so called characteristic frequency (ω_c). The last one is close to the peak frequency in peaked spectra, but more stable in irregular spectra encountered in the archipelago (see Appendix A for the exact definitions of the parameters). As a fourth alternative, which we call ω_d, we took the highest frequency that had a mean direction that differs more than 50° from the estimated wind direction, where 50° tolerates a possible misalignment caused by slanting fetch conditions (Pettersson et al., 2010). Since ω_d is used mostly to discount swell, it is only used if it is below 0.2 Hz.

Since there is more risk to have a too low starting frequency (e.g. dominant swell), we take the highest of the all possibilities, i.e.:

$$\omega_0 = \max\{\omega_p, \omega_m, \omega_c, \omega_d\}. \tag{3}$$

Step 2: We used two restrictions, namely setting a fixed length for the frequency range ($N = 15$ frequency bins, i.e. 0.15 Hz), and setting a highest starting frequency to 1.6 times ω_0. These restrictions are a trade off. A large N gives a more stable

https://doi.org/10.5194/egusphere-2024-3477
Preprint. Discussion started: 25 November 2024

Table 1. The weather conditions during the experiments. Values given for the data used to estimate the wind speed, i.e. H_s>0.3 m and wind directions 180–360° at Sõrve (all directions at Suomenlinna).

Location	Time	U_z	$\langle U_z \rangle$	H_s	$\langle H_s \rangle$	$\langle \frac{\omega_p U}{g} \rangle$	$\langle \frac{\omega_m U}{g} \rangle$
Suomenlinna	11 June 2020 – 4 Nov 2020	1.2–20.0 m s^{-1}	8.6 m s^{-1}	0.30–1.85 m	0.58 m	1.41	1.95
Sõrve	27 July 2021 – 2 Feb 2022	0.3–17.9 m s^{-1}	8.8 m s^{-1}	0.30–3.65 m	1.38 m	1.04	1.35

fit, but also a worse fit if the ω^{-4} range is too short. A high upper limiting frequency can be problematic if the search extends to the ω^{-5} range, but is beneficial if ω_0 happens to be too low.

Step 3: We now have a collection of frequency ranges of length 0.15 Hz that start between ω_0 and $2.0\omega_0$. The best candidate, $\Delta\omega$, must then be chosen based on some metric. We chose the interval that had the smallest root-mean-square logarithmic error (RMSLE, see Appendix B).

Step 4: We can estimate the wind speed from the wave spectrum in $\Delta\omega$ and Eq. (1):

$$U_{10} \approx \left\langle \frac{\hat{S}(\omega)\omega^4}{\alpha_u g} \right\rangle_{\Delta\omega} \tag{4}$$

where U_{10} denotes the wind speed at 10 metre height, $\hat{S}(\omega)$ is the sample spectrum, and $\langle\rangle$ denotes the average. We use a value $\alpha_u = 3.3 - 4.0 \cdot 10^{-3}$ for the experimental constant (Kahma, 1986).

This algorithm follows the one used by Voermans et al. (2020) with some small modifications.

2.3 Wave data

The wave data is from a small spherical wave buoy, LainePoiss®, manufactured by WiseParker OÜ. The device has a diameter less than 0.4 m, weighs less than 5.5 kg and uses accelerometres, a gyroscope and a magnetic compass to measure the wave field. The wave spectra were calculated using the Welch method from 30 minute vertical displacement time series up to 1.28 Hz (8.04 rad s^{-1}). For a more detailed description of both the device, the data, and the data processing procedures, the reader is referred to Alari et al. (2022).

The first wave data set used in this study was gathered in the Finnish archipelago around 4 km from the mainland. The second wave data set was gathered in the Baltic Proper roughly 30 km west of the Estonian island Saaremaa (Fig. 1). For an overview of the wave conditions at the locations during the experiments, see Table 1.

2.4 Wind data

The first wind data set used for validation is from the the Finnish Meteorological Institutes operational weather station that is located at the island Harmaja ca 2 km south of the wave buoy. The weather station provides 10 minute average wind speed and direction, and the wind speeds were reduced to values corresponding to 10 m height by:

https://doi.org/10.5194/egusphere-2024-3477
Preprint. Discussion started: 25 November 2024

Figure 1. The locations of the Helsinki wave buoy (red) and the Saaremaa wave buoy (yellow).

$$U_{10} = U_{z_a} \left(\frac{10}{z_a} \right)^{0.11}, \tag{5}$$

where $z_a = 17.5$ m is the measurement height.

The second wave data set is compared to the results of a numerical hindcast, NORA3 (Haakenstad et al., 2021). The hindcast is based on nonhydrostatic numerical weather prediction model. The hindcast covers the North Sea, the Norwegian Sea, the Barents Sea, and the Baltic Sea, and is a downscaling of the ERA5 reanalysis (Hersbach et al., 2020). The spatial and temporal resolutions of the data are 3 km and 1 h.

For an overview of the wind conditions at the locations during the experiments, see Table 1.

3 Results

3.1 Wind direction retrieval

The simple wind direction retrieval algorithm that estimated the wind direction from the mean direction of wave between 1.00 and 1.28 Hz was robust (Fig. 2). For the data from the archipelago the estimated wind direction was mostly within ±20

https://doi.org/10.5194/egusphere-2024-3477
Preprint. Discussion started: 25 November 2024

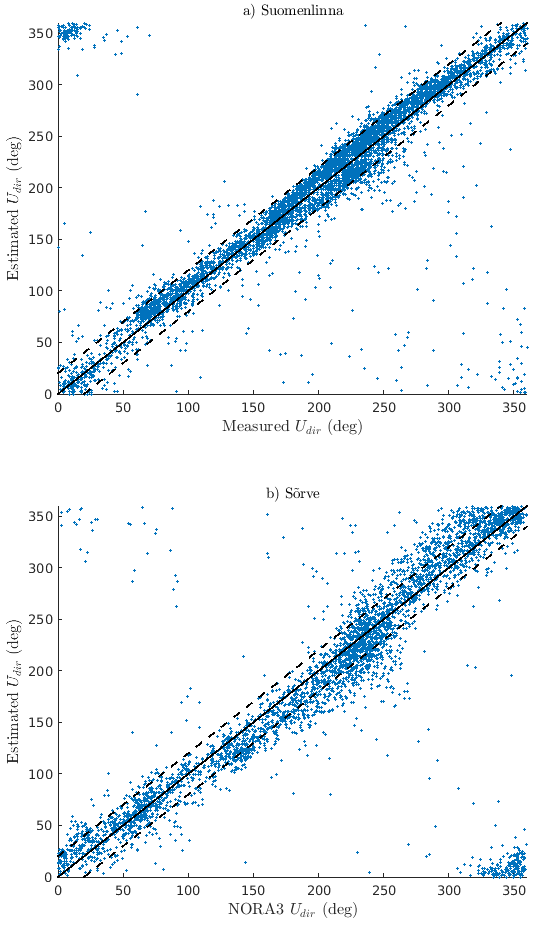

Figure 2. The wind direction estimated from the wave spectra compared to measurements from Harmaja, near the Suomenlinna buoy (top) and the wind direction from the NORA3 hindcast at the Sõrve buoy. Dashed lines show a deviation of ±20 degrees.

degrees of the observed wind which can be considered a good results considering the many islands and proximity to the shoreline. Effects of the shoreline can be seen as systematic biases for certain wind directions.

The estimates from the Baltic Proper has slightly more spread, but the most dominant direction around 200° is estimated well. Most of the data still falls within ±20 degrees.

3.2 Wind speed retrieval

The wind speed inside the archipelago was estimated well using a value of $\alpha_u = 3.3 \cdot 10^{-3}$ (Fig. 3a). The algorithm was unable to retrieve very low wind speeds, but since a wind speed criteria could not be imposed, all data with a significant wave height under 0.3 m were excluded. Higher winds are estimated well, with wind speeds between 15–20 $\mathrm{m\ s^{-1}}$ being slightly underestimated. Nonetheless, the strongest wind speeds come from southwest. From this direction the wave buoy is sheltered

https://doi.org/10.5194/egusphere-2024-3477
Preprint. Discussion started: 25 November 2024

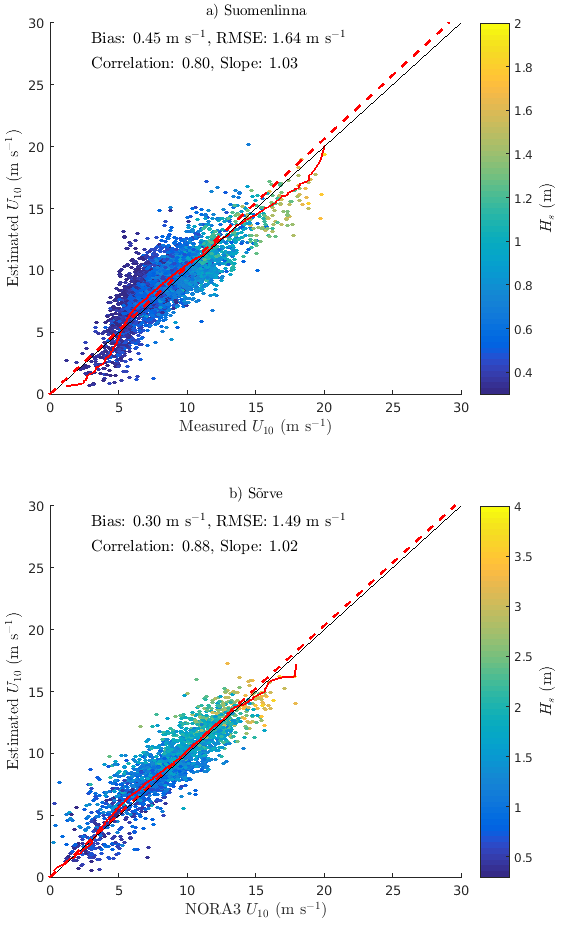

Figure 3. The wind speed estimated from the wave spectra compared to measurements from Harmaja, near the Suomenlinna buoy (top), and the wind direction from the NORA3 hindcast at the Sõrve buoy. The top panel results are calculated using $\alpha_u = 3.3 \cdot 10^{-3}$ and the bottom panel using $\alpha_u = 4.0 \cdot 10^{-3}$. Significant wave heights below 0.3 m are excluded. Red solid lines are quantile lines.

by islands, while the weather station measures more undisturbed conditions. Plotting the bias as a function of the wind direction also reveals systematic differences (Fig. 4). A part of the discrepancy might therefore stem from actual small scale differences in the wind and wave fields.

For the location at Sõrve we excluded winds blowing over land (0–180°). The comparison to the NORA3 hindcast shows that the wind speed in the Baltic Proper was also estimated accurately using a value of $\alpha_u = 4.0 \cdot 10^{-3}$ (Fig. 3b). Here, the highest wind speeds over 15 m s^{-1} show no particular bias, although the data in that wind speed region is sparse.

Using a higher upper limit for the searching algorithm (e.g. 2.0 ω_0 instead of 1.6 ω_0) introduces a curvature leading to an underestimation of the highest wind speeds (not shown). This is caused by the searching algorithm moving past a $\omega^{-4} - \omega^{-5}$ transition into a second ω^{-4} range, with a lower equilibrium level. A similar transition has been recorded also by wave staffs

https://doi.org/10.5194/egusphere-2024-3477
Preprint. Discussion started: 25 November 2024

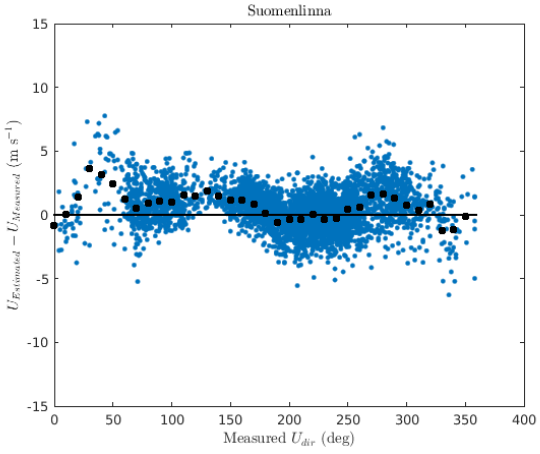

Figure 4. The wind speed bias at Suomenlinna as a function of the observed wind direction. Black dots denote 10 degree averages.

(Björkqvist et al., 2019a). This double transition is more readily seen in the spectra from LainePoiss, which go up to 1.28 Hz instead of the 0.6 Hz upper frequency of the larger Waverider buoys. Nonetheless, since the transitions happen at dimensionless frequencies, this same spectral shape has also been reported in Waverider measurements in a Baltic Sea storm (Björkqvist et al., 2020). This issue might therefore reveal itself in wind speeds above roughly 25 m s^{-1} in measurements going up to around 0.5 Hz.

4 Discussion

The wind speed from the two data sets was estimated using identical settings in the wind speed retrieval algorithm except for the chosen value of the experimental equilibrium constant α_u. A lower value of $3.3 \cdot 10^{-3}$ was found more appropriate in the more sheltered, short fetch, archipelago, while the more exposed Baltic Proper data was better explained by a higher $4.0 \cdot 10^{-3}$ value.

The mean inverse wave age ($\omega_m U/g$ or $\omega_p U/g$) was about 40% higher in the archipelago short fetch data (see Table 1). A lower equilibrium value for a higher inverse wave age was seen qualitatively in the Baltic Sea data of Björkqvist et al. (2019a), and Donelan et al. (1985) has previously quantified a wave age dependence of the equilibrium level. The results of Donelan et al. (1985) can be re-written to the form of Kahma (1981) as presented in out Eq. 1 (see Björkqvist et al. (2019a) Appendix A). The constant α_u will then have the form

$$\alpha_u = 6.0 \cdot 10^{-3} \left(\frac{U}{c_p} \right)^{-0.45}, \tag{6}$$

where $-0.45 = p - 1$ with $p = 0.55$ as determined by Donelan et al. (1985). According to this formula an increase in the inverse wave age with 40%, which we observed in the mean sense, should lead to a *decrease* of the equilibrium constant by

https://doi.org/10.5194/egusphere-2024-3477
Preprint. Discussion started: 25 November 2024

roughly 15%. This is in decent agreement with our chosen values: $\left(4.0 \cdot 10^{-3}\right) \cdot 0.85 = 3.4 \cdot 10^{-3}$, which is close to $3.3 \cdot 10^{-3}$ Nevertheless, trying to implement this functional dependency of Donelan et al. (1985) in the algorithm caused a significant increase in scatter when the inverse wave age was determined per spectrum. The scatter increased especially in the archipelago location and it persisted even if the inverse wave age was determined using a more stable parameters, such as ω_m.

5 Summary and conclusions

An automatic algorithm for detecting wind speed and direction from wave spectra was tested on wave measurements from two locations in the Baltic Sea, collected with a small LainePoiss wave buoy. One was in a sheltered archipelago area, while the other data set was gathered in the exposed Baltic Proper. The wind speeds during the measurement campaigns were up towards $20\ \mathrm{m\ s^{-1}}$.

The wind direction was estimated equally well with identical algorithms for both data sets, and was mostly within 20 degrees of the measured or modelled "ground truth". The wind speed was also estimated accurately with identical algorithm settings except for the value of the experimental α_u equilibrium constant, which was set to an about 20% lower value in the archipelago to get the best fit. The results from previous studies suggest that this might be connected to the short fetch geometry (and therefore higher inverse wave ages) in the archipelago. The discrepancies seem to be beyond what can be corrected for using this algorithm, and we can only recommend that a higher value is used for more exposed conditions.

The small size of the buoy is a clear advantage for estimating the wind direction, since the wave spectrum goes up to 1.28 Hz, and shorter waves are less affected by e.g. slanting fetches. For the wind speed retrieval the high upper frequency is beneficial for lower wind speeds, but can cause an underestimation of the higher wind speeds unless an upper frequency is used for the searching algorithm, as done in this study. We note that this same tendency might become an issue also for larger wave buoys for very high wind speeds, even though it is not visible in data sets containing more moderate wind speeds.

Code and data availability. The Harmaja weather data is publicly available from the FMI open data portal: https://en.ilmatieteenlaitos.fi/open-data. The NORA3 data is publicly available on the MET Norway thredds server: https://thredds.met.no/thredds/projects/nora3.html and it was downloaded using the DNORA software package available at https://github.com/MET-OM/dnora.

.

Appendix A: Definition of wave parameters

We use the following definitions of wave parameters, all integrated over $2\pi 0.05$–$2\pi 1.28\ \mathrm{rad\,s^{-1}}$. The significant wave height:

$$H_s = H_{m_0} = \int S(\omega) \mathrm{d}\omega \tag{A1}$$

https://doi.org/10.5194/egusphere-2024-3477
Preprint. Discussion started: 25 November 2024

The peak wave frequency:

$$\omega_p = \mathrm{argmax}_\omega\{S(\omega)\} \tag{A2}$$

The mean wave frequency:

$$\omega_m = \frac{\int \omega S(\omega)\mathrm{d}\omega}{\int S(\omega)\mathrm{d}\omega} \tag{A3}$$

The characteristic wave frequency:

$$\omega_c = \frac{\int \omega S(\omega)^4\mathrm{d}\omega}{\int S(\omega)^4\mathrm{d}\omega} \tag{A4}$$

The characterisic frequency was proposed as an alternative version of the peak frequency by Young (1995) and Björkqvist et al. (2019b) used it on data from a complex coastal archipelago and showed that is had good, stable properties.

Appendix B: Details of fitting

The goodness of a ω^{-4}-fit was evaluated by calculating the root-mean-squared logarithmic error:

$$\mathrm{RMSLE} = \sqrt{\left\langle \left(\log(S(\omega)+1) - \log(\hat{S}(\omega)+1)\right)^2 \right\rangle} \tag{B1}$$

Where $S(\omega) = \langle \hat{S}(\omega)\omega^4\rangle\omega^{-4}$ is the theoretical ω^{-4} fit to the measured spectrum.

Author contributions. The study was initiated by JVB and VA. The wave data was gathered by VA and the wave data processing was performed by VA and JVB. The wind speed algorithm was coded by JVB and the analysis of the data was performed by JVB. The manuscript was written by JVB with input from VA.

Competing interests. The authors declare that no competing interests are present.

https://doi.org/10.5194/egusphere-2024-3477
Preprint. Discussion started: 25 November 2024

Acknowledgements. This paper was financially supported by the Estonian Development Grant EAG100 funded by the Estonian Research Council and co-funded by the European Union and Estonian Research Council via project TEM-TA38 (Digital Twin of Marine Renewable Energy).

https://doi.org/10.5194/egusphere-2024-3477
Preprint. Discussion started: 25 November 2024

Appendix: References

Alari, V., Björkqvist, J.-V., Kaldvee, V., Mölder, K., Rikka, S., Kask-Korb, A., Vahter, K., Pärt, S., Vidjajev, N., and Tõnisson, H.: LainePoiss — A Lightweight and Ice-Resistant Wave Buoy, Journal of Atmospheric and Oceanic Technology, 39, 573–594, https://doi.org/10.1175/JTECH-D-21-0091.1, 2022.

Banner, M. L.: Equilibrium Spectra of Wind Waves, Journal of Physical Oceanography, 20, 966–984, https://doi.org/10.1175/1520-0485(1990)020<0966:ESOWW>2.0.CO;2, 1990.

Björkqvist, J.-V., Pettersson, H., Drennan, W. M., and Kahma, K. K.: A New Inverse Phase Speed Spectrum of Non Linear Gravity Wind Waves, Journal of Geophysical Research: Oceans, 124, 6097–6119, https://doi.org/10.1029/2018JC014904, 2019a.

Björkqvist, J.-V., Pettersson, H., and Kahma, K. K.: The wave spectrum in archipelagos, Ocean Science, 15, 1469–1487, https://doi.org/10.5194/os-2019-59, 2019b.

Björkqvist, J.-V., Rikka, S., Alari, V., Männik, A., Tuomi, L., and Pettersson, H.: Wave height return periods from combined measurement – model data : a Baltic Sea case study, Natural Hazards and Earth System Sciences, 20, 3593–3609, 2020.

Donelan, M. A., Hamilton, J., and Hui, W. H.: Directional Spectra of Wind-Generated Waves, Philosophical Transactions of the Royal Society A: Mathematical, Physical and Engineering Sciences, 315, 509–562, https://doi.org/10.1098/rsta.1985.0054, 1985.

Forristall, G. Z.: Measurements of a saturated range in ocean wave spectra, Journal of Geophysical Research, 86, 8075–8084, https://doi.org/10.1029/JC086iC09p08075, 1981.

Haakenstad, H., Øyvind Breivik, Furevik, B. R., Reistad, M., Bohlinger, P., and Aarnes, O. J.: NORA3: A Nonhydrostatic High-Resolution Hindcast of the North Sea, the Norwegian Sea, and the Barents Sea, Journal of Applied Meteorology and Climatology, 60, 1443 – 1464, https://doi.org/10.1175/JAMC-D-21-0029.1, 2021.

Hersbach, H., Bell, B., Berrisford, P., Hirahara, S., Horányi, A., Muñoz-Sabater, J., Nicolas, J., Peubey, C., Radu, R., Schepers, D., Simmons, A., Soci, C., Abdalla, S., Abellan, X., Balsamo, G., Bechtold, P., Biavati, G., Bidlot, J., Bonavita, M., De Chiara, G., Dahlgren, P., Dee, D., Diamantakis, M., Dragani, R., Flemming, J., Forbes, R., Fuentes, M., Geer, A., Haimberger, L., Healy, S., Hogan, R. J., Hólm, E., Janisková, M., Keeley, S., Laloyaux, P., Lopez, P., Lupu, C., Radnoti, G., de Rosnay, P., Rozum, I., Vamborg, F., Villaume, S., and Thépaut, J.-N.: The ERA5 global reanalysis, Quarterly Journal of the Royal Meteorological Society, 146, 1999–2049, https://doi.org/https://doi.org/10.1002/qj.3803, 2020.

Holthuijsen, L. H.: Observations of the Directional Distribution of Ocean-Wave Energy in Fetch-Limited Conditions, Journal of Physical Oceanography, 13, 191–207, https://doi.org/10.1175/1520-0485(1983)013<0191:OOTDDO>2.0.CO;2, 1983.

Janssen, P. A.: Wave-Induced Stress and the Drag of Air Flow over Sea Waves, Journal of Physical Oceanography, 19, 745–754, https://doi.org/10.1175/1520-0485(1989)019<0745:WISATD>2.0.CO;2, 1989.

Jiang, H.: Wind speed and direction estimation from wave spectra using deep learning, Atmospheric Measurement Techniques, 15, 1–9, https://doi.org/10.5194/amt-15-1-2022, 2022.

Kahma, K. K.: A Study of the Growth of the Wave Spectrum with Fetch, Journal of Physical Oceanography, 11, 1503–1515, https://doi.org/10.1175/1520-0485(1981)011<1503:ASOTGO>2.0.CO;2, 1981.

Kahma, K. K.: On prediction of the fetch-limited wave spectrum in steady wind, Finnish Marine Research, 253, 53–78, 1986.

Kitaigorodskii, S. A.: On the Theory of the Equilibrium Range in the Spectrum of Wind-Generated Gravity Waves, Journal of Physical Oceanography, 13, 816–827, https://doi.org/10.1175/1520-0485(1983)013<0816:OTTOTE>2.0.CO;2, 1983.

https://doi.org/10.5194/egusphere-2024-3477
Preprint. Discussion started: 25 November 2024

Kuik, A. J., van Vledder, G. P., Holthuijsen, L. H., and Vledder, G. P. v.: A Method for the Routine Analysis of Pitch-and-Roll Buoy Wave Data, Journal of Physical Oceanography, 18, 1020–1034, https://doi.org/10.1175/1520-0485(1988)018<1020:AMFTRA>2.0.CO;2, 1988.

Pettersson, H., Kahma, K. K., and Tuomi, L.: Wave Directions in a Narrow Bay, Journal of Physical Oceanography, 40, 155–169, https://doi.org/10.1175/2009JPO4220.1, 2010.

Phillips, O. M.: The equilibrium range in the spectrum of wind-generated waves, Journal of Fluid Mechanics, 4, 426–434, https://doi.org/10.1017/S0022112058000550, 1958.

Phillips, O. M.: Spectral and statistical properties of the equilibrium range in wind-generated gravity waves, Journal of Fluid Mechanics, 156, 505–531, https://doi.org/10.1017/S0022112085002221, 1985.

Resio, D., Long, C. E., and Vincent, C. L.: Equilibrium-range constant in wind-generated wave spectra, Journal of Geophysical Research, 109, 1–14, https://doi.org/10.1029/2003JC001788, 2004.

Toba, Y.: Local Balance in the Air–Sea Boundary Processes III. On the Spectrum of Wind Waves, Journal of the Oceanographical Society of Japan, 29, 209–220, https://doi.org/10.1007/BF02109506, 1973.

Voermans, J. J., Smit, P. B., Janssen, T. T., and Babanin, A. V.: Estimating Wind Speed and Direction Using Wave Spectra, Journal of Geophysical Research: Oceans, 125, 1–16, https://doi.org/10.1029/2019JC015717, 2020.

Young, I. R.: The determination of confidence limits associated with estimates of the spectral peak frequency, Ocean Engineering, 22, 669–686, https://doi.org/10.1016/0029-8018(95)00002-3, 1995.